



J. Serb. Chem. Soc. 91 (0) 1–13 (2026)
JSCS–13645

Investigation of morphological and mechanical properties of hardened and tempered AISI 4340 steel

SUBHAN ALI^{1*}, ABDUL QADEER LAGHARI^{2**}, ARSHAD IQBAL³, GHULAM MUSTAFA MEMON⁴, IFITKHAR AHMED MEMON¹, FIDA HUSSAIN CHANNA⁵, ABDUL SAMI CHANNA⁶, MASROOR ABRO², KHAN MUHAMMAD³ and SHOUKAT ALI NOONARI⁷

¹Materials Engineering Department, Dawood University of Engineering and Technology, Karachi, 74800, Sindh, Pakistan, ²Chemical Engineering Department, Mehran University of Engineering and Technology, Jamshoro, 76080, Pakistan, ³Chemical Engineering Department, Dawood University of Engineering and Technology, Karachi, 74800, Sindh, Pakistan, ⁴IRC for Industrial Nuclear Energy, King Fahd University of Petroleum & Minerals, Saudi Arabia, ⁵Mining Engineering Department, Mehran University of Engineering and Technology, Jamshoro, 76080, Pakistan, ⁶Chemical Engineering Department, Qaid-e-Awam University of Engineering and Technology, Nawabshah, 74800, Pakistan and ⁷Department of Mechanical Engineering, Isra University, Hyderabad, Sindh, Pakistan

(Received 23 November, revised 26 December 2025, accepted 9 March 2026)

Abstract: AISI 4340 steel is widely used in risk-intensive industries due to its excellent mechanical strength and impact resistance. The mechanical properties of AISI 4340 steel can be significantly enhanced through heat treatment, particularly tempering at controlled temperatures. This study investigates the effect of tempering on the microstructure and mechanical properties of AISI 4340 steel. The experimental analysis includes characterization before and after heat treatment to assess changes in strength, toughness and ductility. The results demonstrate that tempering at 450 °C for 45 min provides the optimum balance of impact energy and ductility while slightly reducing hardness and strength. Conversely, tempering at 550 °C results in a more pronounced increase in impact energy and ductility, but at the cost of a greater reduction in hardness and strength. Microstructural examination confirms the formation of tempered martensite, contributing to the observed mechanical behaviour. The findings provide valuable insights into optimizing heat treatment parameters for AISI 4340 steel to achieve a balanced combination of strength, toughness, and ductility for industrial applications.

Keywords: AISI 4340 steel; tempering; mechanical properties; heat treatment.

*,** Corresponding authors. E-mail: (*)subhan.jogi@duet.edu.pk,
(**)abdul.qadeer@admin.muet.edu.pk
<https://doi.org/10.2298/JSC251123012A>

INTRODUCTION

Low alloy AISI 4340 steel has found application in the military sector, critical aircraft components, and nuclear power plants, attributable to its mechanical properties such as tensile strength, stiffness, exceptional processability, optimal hardness and improved weldment.^{1,2} Nickel in steel, compared to that in other medium and low alloy steels, enhances tensile toughness and hardness.³ It has been reported that high-strength steels used in industries suffer from unexpected brittle failure.⁴ The catastrophic failure of engineering components under service conditions, shutdown of power plants, and elevated impairment costs of engineering machine components are serious consequences during operation.^{5,6} Dual-phase steel structures produced by various means have been planned nowadays for the proud performance of structural steel.⁷ Reported work clarified the effect of quenching and tempering treatments for optimising properties of AISI 4340 steel.⁸ Additionally, quenching and tempering treatments significantly increase the ultimate tensile strength of the steel.⁹ Published work rectified that quenching and tempering heat treatment can be used to develop the tempered martensitic steel.¹⁰ Moreover, the hardening treatment of AISI 4340 steel substantially increases the toughness and minimised brittle fracture.^{11,12} Furthermore, recommendations regarding the toughness and strength of AISI 4340 steel indicate that the heat treatments for homogenization, normalizing, quenching and tempering, inter-critical annealing, austempering and martempering may be required.¹³ Subsequently, it was demanded that the upgrading of mechanical properties of AISI 4340 steel by numerous heat treatments procedures and by controlled metal-forming processes.¹⁴ Likewise, an inter-critical quenching process was applied to produce austenite phase for TRIP steel.¹⁵ Nevertheless, difficulties in metal forming processes and high operating equipment costs in process industries. In alternative, it was conveyed that a substantial alteration in the mechanical properties of steel is achieved by intermediate quenching treatment.¹⁶ For the advancement of AISI 4340 steel is used in quench and temper form, though, it is susceptible to embrittlement when tempered at temperatures ranging from 300 to 400 °C.¹⁷ The embrittlement problems addressed by many researchers in their findings that changes in micrographs and mechanical properties at diverse tempering temperatures.¹⁸ Temper heat treatment can be used as a stress relief procedure, confirming reduction of tensile residual stresses, which have badly influence on fatigue life of components.¹⁹ Despite widespread usage in industries of AISI 4340 steel and detailed study of the mechanical performance of the material, there is little published work in literature about the effect of heat treatment parameters on residual stresses.²⁰ The objective of the present work is to optimise mechanical properties of steel AISI 4340 through hardening treatment. The hardening method improves the strength and stiffness of materials by treating them at a specified temperature followed by quenching in water and oil medium.²¹

Temper treatment practice in ferrous materials is useful after hardening.²² In tempering procedure, steel is subjected to heating and cooling below the transformation temperature range and takes time for cooling at a suitable rate.²³ Tempering treatment causes of reduction in hardness and increases the toughness to get the desired mechanical properties.^{24,25} Hence, in current study, AISI 4340 high strength low alloy steel has been designated and treated at suitable temperature to stabilize the microstructure for optimisation of mechanical properties. AISI 4340 steel applied in machine components, but it is required for service conditions in various forms extending from aircraft structures to automotive crankshafts, where diverse characteristics are required.²⁶ In this study, hardening and tempering techniques are employed to alter the mechanical properties and microstructure of AISI 4340 high strength low alloy steel through heat treatment. In addition, outcomes of this research were compared with conventional hardening and tempering of steel. Conclusively, the optimal conditions for attaining the highest toughness were achieved.

EXPERIMENTAL PROCEDURE

Material

Work material for the heat-treatment procedure was made by partitioning AISI 4340 steel bar into cross-sectional areas of 0.621 m² and 0.914 m length. The material in the form of a billet is rolled into a round bar and then cooled in air during the manufacturing procedure of AISI 4340 steel in an industrial unit (Fig. 1).

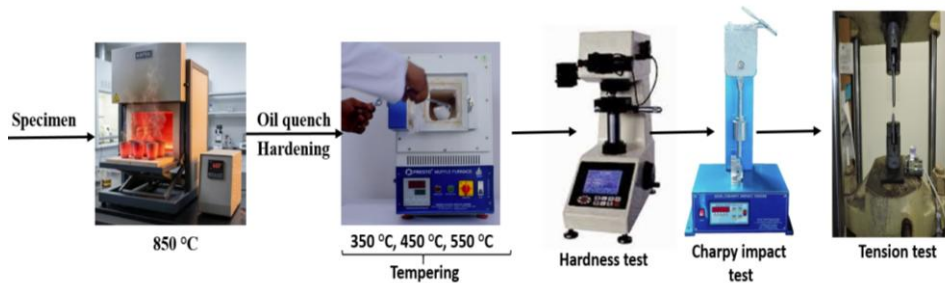


Fig. 1. Experimental setup of AISI 4340 steel bar.

Chemical configuration

The surface of the specimen was prepared by grinding followed by polishing to eliminate surface particles and additional contamination. An optical emission spark spectrometer was used to determine the chemical elements present in the samples. Argon gas was used as an inert atmosphere gas medium through a purifier in the spectrometer. After argon gas stabilization, the specimen was positioned on an anvil and clamped.²⁷ A minimum of three sparks per specimen were made on different positions of the polished surface to determine the average values and standard deviation. Percentage of the elements present in AISI 4340 steel at the initial stage of the study is discussed in Table I.²⁸

TABLE I. Chemical analysis of AISI 4340 steel before heat treatment

| Element | C | Si | Mn | Cr | Mo | Ni | T | Cu | Co | P | S | Fe |
|---------|------|------|------|------|------|------|------|------|-------|-------|-------|---------|
| wt. % | 0.37 | 0.25 | 0.70 | 0.82 | 0.02 | 0.11 | 0.14 | 0.15 | 0.006 | 0.016 | 0.019 | Balance |

Heat treatment procedure

The standard specimens for the impact and tensile tests were prepared from the round bars of AISI 4340 steel placed in a muffle furnace for hardening at 850 °C for 45 min, followed by oil quenching in mineral oil. The hardened heat-treated work material was tempered at 350, 450 and 550 °C and allowed to cool to room temperature.

Hardness testing trials

Hardened and tempered samples were investigated by using a Vickers hardness testing machine HM-100 Series (HV-100), Japan, to measure the resistance to indentation.²⁹ Indentation was made on well-prepared specimens. A 20 kg load was applied for indentation, and the indentations were examined using a microscope. Indentation was measured at an appropriate distance from the sample edge to avoid any edge effects. Three different measurements were made to identify the hardness value of the standard specimen.

Charpy impact testing technique

Impact testing for energy absorption of heat-treated samples was conducted by applying the force of a swinging pendulum. The geometry of the specimens for the Charpy impact test was in accordance with ASTM standard E23 using a Charpy impact testing machine XJJD-50 China.³⁰ The specimens were prepared according to ASTM standard E23.

Tension testing

In the tension test, standard samples were fixed in the grips of the tensile testing machine (ZwickRoell SE-250KN, ZwickRoell Group, Germany) equipped with an electronic load cell. The upper crosshead of the tension testing machine dragged the specimens upward to failure with a constant crosshead speed of 10 mm s⁻¹, to maintain a preliminary strain rate of 2.8 × 10⁻⁴. The stress-strain diagram showed the mechanical properties such as yield strength, ultimate tensile strength and toughness before fracture. The dimension of tensile test samples were in accordance with ASTM standard E8.³¹

RESULTS AND DISCUSSION

AISI 4340 steel in the as-received condition

At first, the chemistry of AISI 4340 steel was analysed and given in Table II. In the chemical analysis, it was evident that 0.82 % Cr is an alloying element present in the steel to enhance resistance against degradation. The strength, toughness, hardness (30 kg load), energy absorption, and tensile properties of the initial samples are presented in Table II.

TABLE II. Mechanical properties of the work material before treatment

| Material | HVN (30 kg) | Impact <i>E</i> J | UTS MPa | Breaking stress MPa | Elongation % |
|----------------------------|----------------|----------------------|------------|------------------------|-----------------|
| AISI 4340 before treatment | 135 | 9.5 | 715 | 468.73 | 33.92 |

Pictorial views of as-received samples of AISI 4340 steel confirm the identification of ferrite structure and pearlite phase in microstructural examination, and the lighter phase corresponds to ferrite. Micrographs were recorded *via* a light optical microscope.

Heat treatment

This contemporary study is capable of enhancing the energy absorption and strength of AISI 4340 low-strength high-alloy steel *via* heat treatment processes; consequently, once the work pieces were ready for mechanical characterization. At the beginning selected samples were subjected to hardening at 850 °C for 45 min and followed by quenching. Secondly, the specimens were tempered at 350, 450 and 550 °C for 45 min and quenched in air.^{32,33}

Hardening procedure of AISI 4340 steel

Following the hardening heat treatment of AISI 4340 steel, it was found that Vickers hardness values increased considerably to 625 (30 kg), whereas the absorbed energy and internal reactive force decreased to 7.53 J and 1520 MPa, respectively. The hardening of AISI 4340 steel reduced the ductility and increased the brittleness. The micrograph contains very fine-grained martensitic regions. Since martensitic regions have a BCT crystal structure and are considered as the hardest phase.³⁴ The pictorial views of the hardening treatment have good agreement with the outcomes reported previously.

Tempering technique of AISI 4340 steel

Tempering treatment after the hardening procedure improves the strength and ductility of the martensitic phase structure of AISI 4340 steel, whereas decreases the hardness.³⁵ Findings of tempering heat treatment are arranged in tabular form Table III. Statistical analysis of the mechanical properties of the materials (AISI 4340 steel) is presented in the comparative graph shown in Fig. 2.

TABLE III. Mechanical properties of the work material after temper treatment

| Material | Tempering temp., °C | HVN (30 kg) | Impact <i>E</i> J | UTS MPa | Elongation % |
|----------|---------------------|----------------|----------------------|------------|-----------------|
| AISI4340 | 350 | 232.6 | 10.49 | 1400.69 | 22.59 |
| | 450 | 219 | 20 | 1456.98 | 29.32 |
| | 550 | 198.13 | 39 | 1255.07 | 30.99 |

It was discovered that the toughness and hardness of the work material are affected by heating in a furnace for hardening and followed by tempering at different temperature levels. Hardening treatment achieved the utmost hardness and tensile strength and reduced the percentage elongation.³⁶ As reported by researchers, the phase change of AISI 4340 steel might be due to the quenching

route, where abrupt changes occur in crystal structure phase from gamma (γ), *i.e.*, FCC to BCT and a martensitic phase structure.³⁷ Rapid intensification in Vickers hardness and strengths occurs during transformation in platelets of the martensite phase, producing enormous alteration, and the same trend was also observed on similar materials.³⁸ It can be seen from the tempering results that improvement of hardness, ultimate strength and toughness is shown in Fig. 2.

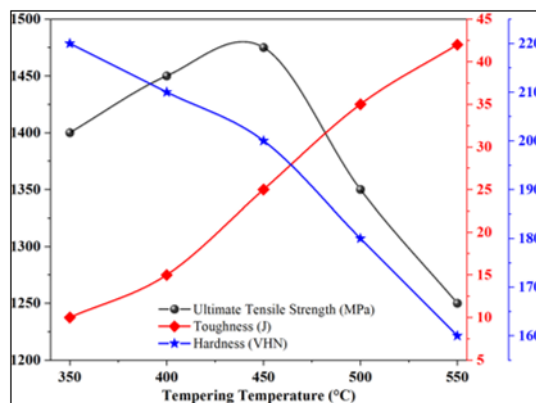


Fig. 2. Comparative analysis of mechanical properties after tempering of hardened AISI 4340 steel at 350–550 °C for 45 min.

The comparative analysis of the heat-treatment results showed that hardness and strength were drastically reduced from 625 to 232.6 *HVN* at 30 kg, and from 1520 to 1400.69 MPa, respectively, whereas the energy absorption increased from 7.53 to 10.49 J. Based on the results, it can be concluded that internal stresses produced by changes in martensitic morphology and contributed to improved ductility. Moreover, a notable change in mechanical properties of the AISI4340 steel was obtained after tempering at 450 °C for 45 min. Furthermore, analysis of the data after heat treatment of AISI 4340 steel showed a decline in hardness values and an increase in strengths and toughness. This can be attributed to the fact that the section was tempered at 550 °C for the same duration, resulting in a decrease in hardness and tensile strength but an increase in toughness. Hence, tempering heat treatment practice of AISI 4340 steel at 450 °C achieves an optimum balance of hardness, tensile strength and toughness.¹³ Experimental evidence shows that low-carbon Mn–Si–Cr steel, when quenched after the hardening procedure, causes phase conversion and affects the mechanical properties.

Scanning electron microscopy analysis

High-strength low-alloy steel is designed particularly for space shuttle, aircraft, and missile structures for defence applications. AISI 4340 steel was subjected to heating and cooling processes to improve fracture resistance and enhance tensile strengths. By heat treatment, the mechanical strength properties of high

strength low alloy steel were modified through tempering and subsequent quenching.³⁹ Phase change of steel occurs by the hardening and tempering technique. The transformed microstructures, like retained austenite, lower bainite, martensite and some carbides, were recognized by means of a high-resolution transmission electron microscope.⁴⁰ It can also be discussed that retained austenite is capable of arresting crack propagation and increases resistance to fracture of low alloy medium carbon steel. Furthermore, research findings indicate that the cracks traveling through martensite are impassable while passing through a region of retained austenite. If internal reactive forces are present, cracks harvest the branches and started to increase close to austenite region, therefore more energy is absorbed through the martensite plates and this promotes the toughness of steel. AISI 4340 steel containing lower bainite and tempered martensite as a dual phase is extensively studied concerning its mechanical properties. It is notified that the dual-phase steel provides a healthier combination of strength and toughness compared with wholly martensitic structures.⁴¹ discussed previously from the optical micrographs, detailed information regarding variations occurring through the phase alteration process was required, hence, it was found essential to inspect hardened and tempered work pieces by using SEM. The micrograph in Fig. 3a shows evidence of a dual-phase microstructure containing lower bainite and martensitic structure of AISI 4340 steel tempered at a temperature of 350 °C for 45 min. The SEM microstructure captured at high resolution and magnification is displayed in Fig. 3b, showing a dual-phase microstructure of lower bainite and martensite plates layered with an austenitic phase structure on the grain boundaries. A comparable topography was detected (Fig. 3c and d), for the specimens inspected with high resolution SEM after tempering at 450 and 550 °C for 45 min.

In this contemporary study, a steel grade was hardened and tempered to reduce the hardness associated with martensitic structure while enhancing the high-energy region. It has been testified by numerous investigators.⁴² that P, S and Sn and antimony have an adverse effect on steel showing a brittle appearance once tempered. Impurities present in the steel tend to segregate near the austenitic region and decohesion across the grain boundaries, which eventually results in inter granular brittle failure. These consequences arise from impurity segregation promoted by tempering treatment of steel at elevated temperature. While the similar steel grade, when quenched from elevated temperature, irregularities within the material do not activate during cooling and therefore reduce the embrittlement mechanism of fracture. As is evident from reported results, tempered specimens failed during tensile test and were studied using a scanning electron microscope. The micrograph shown in Fig. 4a represents the fractured surface of a work piece tempered at 350 °C, scrutinized under a scanning electronic microscope and conforming stress-strain photograph. AISI 4340 sectioned pieces exhibited intergranular fracture, which is characteristic of brittle fracture. Illustration of stress-strain diagram

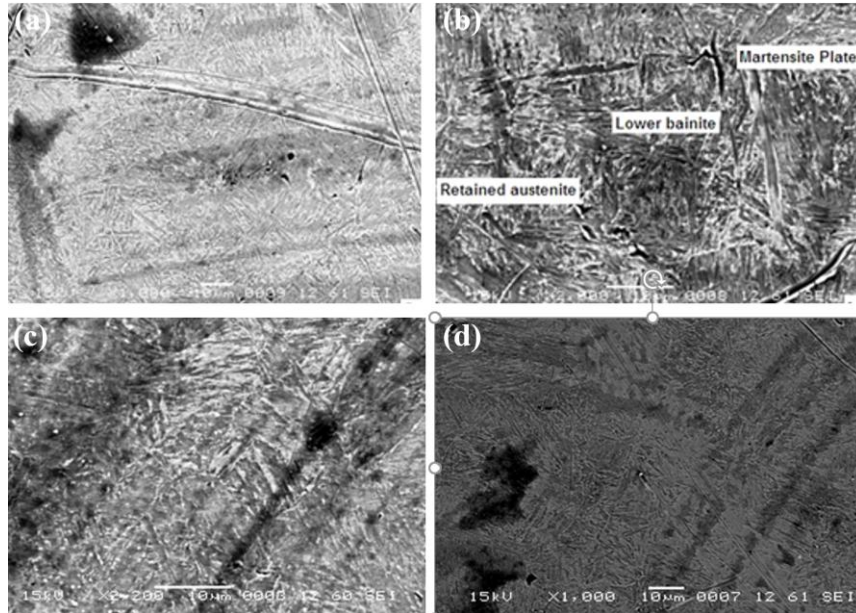


Fig. 3. SEM micrograph of AISI 4340 steel tempered at: a) 350 and b) 450 °C; comparative topography at: c) 450 and d) 550 °C.

did not present any yielding and elongation all through the tensile test. These values indicate brittle fracture material behaviour. Fracture along the grain boundaries of the tempered martensitic phase structure is in good agreement with discoveries conferred previously. New findings quantified in Table IV signify the tempering temperature at 350 °C. The hardness values are comparatively higher and impact energy is relatively lower than the finding of hardness and impact energy noted when tempered at 450 °C. Illustration of Table IV also indicates an increase in tensile strength of the work material. Therefore, the increase in impact energy is accompanied by considerable reduction in the hardness and strength of the specimens.⁴³ Micrographs were recorded for AISI 4340 steel tempered at 350, 450 and 550 °C, as presented in Fig. 4a–c. As the tempering temperature increases, the fracture morphology exhibits a distinct change in failure mode, which is directly correlated with modifications in mechanical behaviour. The fracture surface primarily displays intergranular and quasi-cleavage features in Fig. 4a, which corresponds to tempering at 350 °C. This suggests a relatively brittle fracture mechanism. Tempered martensite with high residual stresses and fine ϵ -carbides, which restrict plastic deformation and encourage crack initiation along previous austenite grain boundaries, is linked to this behaviour. As a result, this condition is usually characterized by increased strength and hardness but reduces toughness. As seen in Fig. 4b, the fracture mode changes towards ductile fracture when the tempering temperature is raised to 450 °C. Microvoid nucleation, growth and coalescence

produce uniformly distributed dimples on the fracture surface. This transition shows increased plasticity as a result of controlled cementite (Fe_3C) precipitation and partial martensitic structure recovery. Strength and toughness are better balanced at this tempering condition, which is frequently regarded as ideal for AISI 4340 steel. The fracture surface exhibits deeper and larger dimples at the maximum tempering temperature of 550 °C (Fig. 4c), indicating a fully ductile fracture mechanism. Carbide coarsening and spheroidisation, as well as substantial stress relief and martensite breakdown into a ferrite–carbide matrix are responsible for the increase in dimple size. This microstructural evolution leads to increased ductility and impact toughness but decreased hardness and strength. The evolution of carbide precipitation Fe_3C and the transformation of the martensitic phase are reflected in the progressive increase in dimple size with tempering temperature. The observed trends in the mechanical properties of tempered and hardened AISI 4340 steel are strongly supported by these morphological changes seen in SEM fractography.

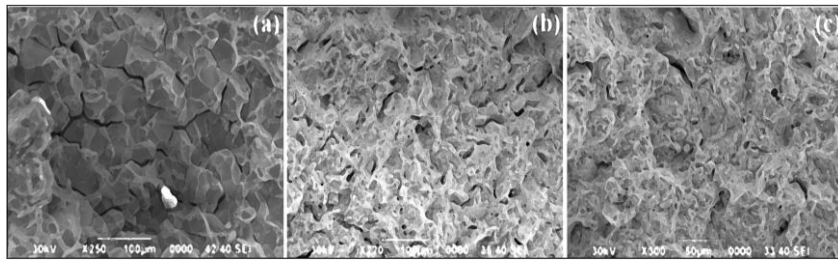


Fig. 4. SEM Analysis of samples after tempering at: a) 350, b) 450 and c) 550 °C.

TABLE IV. Tensile properties of AISI 4340 steel at various tempering temperatures

| Sample | Tempering temp., °C | Diameter (d_0 / mm) | L_0 / mm | F_{max} N/mm ² | F_{Break} % | e_{Break} % | $e-F_{max}$ % |
|--------|---------------------|------------------------|------------|-----------------------------|---------------|---------------|---------------|
| (a) | 350 | 12.5 | 35.08 | 1400.09 | 1400.09 | 22.59 | 22.59 |
| (b) | 450 | 12.5 | 35.14 | 1456.96 | 1186.72 | 36.53 | 29.32 |
| (c) | 550 | 12.5 | 30.07 | 1255.02 | 980.52 | 41.47 | 30.99 |

Table IV presents the tensile properties of three samples subjected to different tempering temperatures (350, 450 and 550 °C), has been fixed by chamber oven UF160-Memmert GmbH+Co. Kg, Germany, highlighting the influence of heat treatment on tensile behaviour. At 350 °C, the sample exhibits a maximum stress of 1400.09 N/mm², Fig. 5, which increases to 1456.96 N/mm² at 450 °C, indicating enhanced strength due to the tempering-induced microstructural changes, such as stress relief and carbide precipitation. However, a further increase in tempering temperature to 550 °C results in a reduction to 1255.02 N/mm², suggesting over-tempering, where coarsening of the microstructure and reduction in dislocation

density lead to decreased strength. A similar trend is observed in the fracture strength, which drops significantly from 1400.09 % at 350 °C to 980.52 % at 550 °C, reflecting a loss in the material's ability to withstand stress before failure as it becomes more ductile. Meanwhile, the elongation at break (e_{Break}) and at maximum stress (e_{Fmax}) increase progressively with tempering temperature, rising from 22.59 % at 350 °C to 41.47 and 30.99 %, respectively, at 550 °C. This indicates a clear enhancement in ductility due to the transformation of the brittle martensitic structure into a more plastic and deformable phase. The results reveal a classic trade-off between strength and ductility with increasing tempering temperature. The sample tempered at 450 °C demonstrates an optimal combination of high tensile strength and improved elongation, suggesting that it may offer the best mechanical performance among the three conditions for applications requiring both durability and formability.

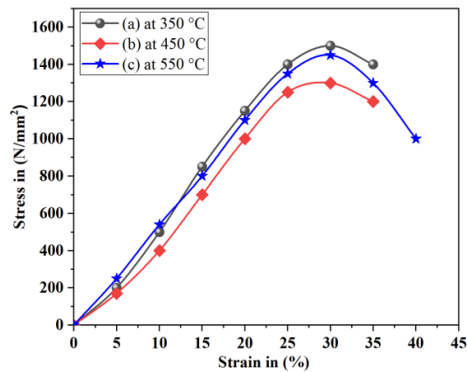


Fig. 5. Illustration of the tensile properties of AISI 4340 steel at different tempering temperatures.

CONCLUSION

This study investigated the tempering of AISI 4340 steel to optimize its mechanical properties, finding that different tempering temperatures yield distinct results. Tempering at 350 °C primarily enhances tensile strength without significantly improving ductility or impact energy, while a higher temperature of 450 °C for 45 min provides an optimal balance, effectively increasing both toughness and ductility while maintaining acceptable levels of strength and hardness. Conversely, tempering at 550 °C leads to a further increase in impact energy and ductility but results in a more significant reduction in strength and hardness. This observed behaviour is directly linked to the formation of tempered martensite within the steel's microstructure, as confirmed by microstructural analysis. Therefore, the findings suggest that a tempering treatment of 450 °C for 45 min is the most effective approach for achieving a desirable combination of mechanical properties for a wide range of engineering applications.

ИЗВОД

ИСПИТИВАЊЕ МОРФОЛОШКИХ И МЕХАНИЧКИХ СВОЈСТАВА КАЉЕНОГ И
ОТПУШТЕНОГ ЧЕЛИКА AISI 4340

SUBHAN ALI¹, ABDUL QADEER LAGHARI², ARSHAD IQBAL³, GHULAM MUSTAFA MEMON⁴, IFITKHAR AHMED MEMON¹, FIDA HUSSAIN CHANNA⁵, ABDUL SAMI CHANNA⁶, MASROOR ABRO², KHAN MUHAMMAD³ и SHOUKAT ALI NOONARI⁷

¹Materials Engineering Department, Dawood University of Engineering and Technology, Karachi, 74800, Sindh, Pakistan, ²Chemical Engineering Department, Mehran University of Engineering and Technology, Jamshoro, 76080, Pakistan, ³Chemical Engineering Department, Dawood University of Engineering and Technology, Karachi, 74800, Sindh, Pakistan, ⁴IRC for Industrial Nuclear Energy, King Fahd University of Petroleum & Minerals, Saudi Arabia, ⁵Mining Engineering Department, Mehran University of Engineering and Technology, Jamshoro, 76080, Pakistan, ⁶Chemical Engineering Department, Qaid-e-Awam University of Engineering and Technology, Nawabshah, 74800, Pakistan и ⁷Department of Mechanical Engineering, Isra University, Hyderabad, Sindh, Pakistan

Челик AISI 4340 се због своје изврсне механичке чврстоће и отпорности на удар широко користи у индустријама високог ризика. Механичка својства овог челика могу се значајно побољшати термичком обрадом, нарочито отпуштањем на контролисаним температурама. Ова студија истражује утицај отпуштања на микроструктуру и механичка својства челика AISI 4340. Експериментална анализа обухвата карактеризацију пре и после термичке обраде како би се процениле промене у чврстоћи, жилавости и дуктилности. Резултати испитивања показују да отпуштање на 450 °C (45 min) оптимално побољшава енергију удара и дуктилност, уз благо смањење тврдоће и чврстоће, док отпуштање на 550 °C доводи до израженијег повећања енергије удара и дуктилности, али по цену већег смањења тврдоће и чврстоће. Микроструктурна испитивања потврђују формирање отпуштеног мартензита, што доприноси уоченом механичком понашању. Ови налази пружају драгоцен увид у оптимизацију параметара термичке обраде челика AISI 4340 ради постизања баланса чврстоће, жилавости и дуктилности за индустријску примену.

(Примљено 23. новембра, ревидирано 26. децембра 2025, прихваћено 9. марта 2026)

REFERENCES

1. S. M. Safi, M. K. B. Givi, *Met. Sci. Heat Treat.* **56** (2014) 78 (<https://doi.org/10.1007/s11041-014-9707-z>)
2. C. Aygüzer, *MSc Thesis*, Middle East Technical University, Turkey, 2023, (<https://hdl.handle.net/11511/107732>)
3. L. Sharma, R. Chhibber, *Proc. Inst. Mech. Eng. E: J. Process Mech. Eng.* **235** (2021) 266 (<https://doi.org/10.1177/0954408920958104>)
4. L. Moravcikova-Gouvea, I. Moravcik, M. Omasta, J. Veselý, J. Cizek, P. Minárik, J. Cupera, A. Záděra, V. Jan, I. Dlouhy, *Mater. Charact.* **159** (2020) 110046 (<https://doi.org/10.1016/j.matchar.2019.110046>)
5. T. Siostrzonek, J. Wójcik, M. Dutka, W. Siostrzonek, *Energies* **17** (2024) 5675 (<https://doi.org/10.3390/en17225675>)
6. K. M. Groth, A. Al-Douri, M. West, K. Hartmann, G. Saur, W. Buttner, *Int. J. Hydrogen Energy* **51** (2024) 1023 (<https://doi.org/10.1016/j.ijhydene.2023.07.165>)
7. A. Fande, S. Kavishwar, V. Tandon, D. C. Narayane, D. Bandhu, *Mater. Res. Express.* **11** (2024) 056519 (<https://doi.org/10.1088/2053-1591/ad4bab>)

8. R. Seede, B. Zhang, A. Whitt, S. Picak, S. Gibbons, P. Flater, A. Elwany, R. Arroyave, I. Karaman, *Addit. Manuf.* **47** (2021) 102255 (<https://doi.org/10.1016/j.addma.2021.102255>)
9. Y. Zhang, J. Yang, D. Xiao, D. Luo, C. Tuo, H. Wu, *Metals* **12** (2022) 1087 (<https://doi.org/10.3390/met12071087>)
10. F. Deirmina, N. Peghini, B. AlMangour, D. Grzesiak, M. Pellizzari, *Mater. Sci. Eng., A* **753** (2019) 109 (<https://doi.org/10.1016/j.msea.2019.03.027>)
11. F. Hosseinifar, A. Ekrami, *Mater. Sci. Eng., A* **830** (2022) 142314 (<https://doi.org/10.1016/j.msea.2021.142314>)
12. A. Khodabandeh, D. Sayadi, S. Rajabi, M. Khosrojerdi, M. Khajehzadeh, M. R. Razfar, *Proc. Inst. Mech. Eng., C.: J. Mech. Eng. Sci.* **238** (2024) 7607 (<https://doi.org/10.1177/09544062241232236>)
13. M. Parvinzadeh, S. S. Karganroudi, N. Omid, N. Barka, M. Kh Int. *J. Adv. Manuf. Technol.* **115** (2021) 1 (<https://doi.org/10.1007/s00170-021-07351-5>)
14. M. K. Sanij, S. G. Banadkouki, A. Mashreghi, M. Moshrefifar, *Mater. Des.* **42** (2012) 339 (<https://doi.org/10.1016/j.matdes.2012.06.017>)
15. A. Kokosza, J. Pacyna, *Arch. Metall. Mater.* **59** (2014) 1017 (<https://doi.org/10.2478/amm-2014-0170>)
16. I. Dey, R. Saha, B. Mahato, M. Ghosh, S. Ghosh, *Metall. Mater. Trans., A* **55** (2024) 1 (<https://doi.org/10.1007/s11661-024-07431-7>)
17. M. de Souza, L. F. Serrão, J. M. Pardal, S. S. M. Tavares, M. C. Fonseca, *Int. J. Adv. Manuf. Technol.* **120** (2021) 1123 (<https://doi.org/10.1007/s00170-022-08880-3>)
18. S. Sharma, J. Singh, M. K. Gupta, M. Mia, S. P. Dwivedi, A. Saxena, S. Chattopadhyaya, R. Singh, D. Y. Pimenov, M. E. Korkmaz, *J. Mater. Res. Technol.* **12** (2021) 1564 (<https://doi.org/10.1016/j.jmrt.2021.03.095>)
19. M. Kumaran, S. Ravi, *Mater. Lett.* **377** (2024) 137427 (<https://doi.org/10.1016/j.matlet.2024.137427>)
20. D. Schröpfer, A. Kromm, T. Lausch, M. Rhode, R. Wimpory, T. Kannengießler, *Weld. World.* **14** (2021) 1 (<https://doi.org/10.1007/s40194-021-01101-7>)
21. J. Yang, Z. Zhu, S. Han, Y. Gu, Z. Zhu, H. Zhang, *J. Alloys Compd.* **1008** (2024) 176707 (<https://doi.org/10.1016/j.jallcom.2024.176707>)
22. T. Sonar, S. Lomte, C. Gogte, *Mater. Today: Proc.* **5** (2018) 25219 (<https://doi.org/10.1016/j.matpr.2018.10.324>)
23. V. S. J. Milton, Z. C. J. Wilmer, H. A. D. Bryan, Z. C. J. Gregorio, Á. R. A. Linzan, M. E. C. Guaigua, A. C. Z. Rodríguez, *Nanotechnol. Perceptions* **20** (2024) 307 (<https://doi.org/10.62441/nano-ntp.vi.408>)
24. E. Tkachev, S. Borisov, A. Belyakov, T. Kniaziuk, O. Vagina, S. Gaidar, R. Kaibyshev, *Mater. Sci. Eng., A* **868** (2023) 144757 (<https://doi.org/10.1016/j.msea.2023.144757>)
25. A. Panda, R. Bag, A. K. Sahoo, R. Kumar, *Int. J. Integr. Eng.* **12** (2020) 61 (<https://publisher.uthm.edu.my/ojs/index.php/ijie/article/view/5667>)
26. A. Saboori, A. Aversa, G. Marchese, S. Biamino, M. Lombardi, P. Fino, *Appl. Sci.* **9** (2019) 3316 (<https://doi.org/10.3390/app9163316>)
27. J. Miao, L.-l. Yu, X.-g. Liu, B.-f. Guo, *Trans. Nonferrous Met. Soc. China* **28** (2018) 2082 ([https://doi.org/10.1016/S1003-6326\(18\)64852-6](https://doi.org/10.1016/S1003-6326(18)64852-6))

28. J. Yan, C. Zhang, J. Guo, G. Dong, S. Wang, J. Gao, H. Wu, H. Zhao, J. Lu, Y. Huang, X. Mao, *J. Mater. Res. Technol.* **38** (2025) 3264 (<https://doi.org/10.1016/j.jmrt.2025.08.142>)
29. M. A. Hafeez, M. Usman, M. A. Arshad, M. AdeelUmer, *Crystals* **10** (2020) 508 (<https://doi.org/10.3390/cryst10060508>)
30. L. F. Monaheng, W. B. du Preez, C. Polese, *Metals* **11** (2021) 1736 (<https://doi.org/10.3390/met11111736>)
31. J. Na, J. Middendorf, M. Lander, J. Waller, R. Rauser, in *Structural Integrity of Additive Manufactured Parts*, N. Shamsaei, S. Daniewicz, N. Hrabe, S. Beretta, J. Waller, M. Seifi, Eds., ASTM International, West Conshohocken, PN, 2020, p. 206 (<https://doi.org/10.1520/STP162020180095>)
32. S. Bakhshi, M. Asadi Asadabad, S. Bakhshi, S. Bakhshi, *Ironmak. Steelmak.* **50** (2023) 295 (<https://doi.org/10.1080/03019233.2022.2107111>)
33. S. Khatai, A. K. Sahoo, R. Kumar, A. Panda, *Proc. Inst. Mech. Eng., C: J. Mech. Eng. Sci.* **238** (2024) 10997 (<https://doi.org/10.1177/09544062241276347>)
34. W. Tan, , *PhD Thesis*, New York State College of Ceramics at Alfred University, 2017, (<http://hdl.handle.net/10829/24629>)
35. M. M. Bilal, K. Yaqoob, M. H. Zahid, W. H. Tanveer, A. Wadood, B. Ahmed, *J. Mater. Res. Technol.* **8** (2019) 5194 (<https://doi.org/10.1016/j.jmrt.2019.08.042>)
36. S. Sharma, A. Kini, G. Shankar, T. Rakesh, H. Raja, K. Chaitanya, M. Shettar, *J. Mech. Eng. Sci.* **12** (2018) 3866 (<https://doi.org/10.15282/jmes.12.3.2018.8.0339>)
37. A. F. Brust, *PhD Thesis*, Ohio State University, 2019 (http://rave.ohiolink.edu/etdc/view?acc_num=osu155523646156822)
38. M. Motyka, *Metals* **11** (2021) 481 (<https://doi.org/10.3390/met11030481>)
39. F. P. Li, N. Li, X. L. Wang, M. H. Liang, *Mater. Sci. Forum* **1035** (2021) 424 (<https://doi.org/10.4028/www.scientific.net/MSF.1035.424>)
40. X. Wang, C. Liu, Y. Qin, Y. Li, Z. Yang, X. Long, M. Wang, F. Zhang, *Mater. Sci. Eng., A* **832** (2022) 142357 (<https://doi.org/10.1016/j.msea.2021.142357>)
41. M. Elitas, *Mater. Test.* **63** (2021) 124 (<https://doi.org/10.1515/mt-2020-0019>)
42. G. Muthukumaran, P. D. Babu, *Arab. J. Sci. Eng.* **1008** (2022) 1 (<https://doi.org/10.1007/s13369-021-06350-8>)
43. F. A. Khatir, M. H. Sadeghi, S. Akar, *J. Manuf. Process.* **61** (2021) 173 (<https://doi.org/10.1016/j.jmapro.2020.09.073>).